

# 1

## The Chemistry of Arsenic, Antimony and Bismuth

*Neil Burford, Yuen-ying Carpenter, Eamonn Conrad and Cheryl D.L. Saunders*

*Department of Chemistry, Dalhousie University, Halifax, Nova Scotia, B3H 4J3, Canada*

Arsenic, antimony and bismuth are the heavier pnictogen (Group 15) elements and consistent with their lighter congeners, nitrogen and phosphorus, they adopt the ground state electron configuration  $ns^2np^3$ . Arsenic and antimony are considered to be metalloids and bismuth is metallic, while nitrogen and phosphorus are non-metals. Arsenic and antimony are renowned for their toxicity or negative bioactivity [1, 2] but bismuth is well known to provide therapeutic responses or demonstrate a positive bioactivity [3]. As a background to the biological and medicinal chemistry of these elements, the fundamental chemical properties of arsenic, antimony and bismuth are presented in this introductory chapter.

### 1.1 Properties of the Elements

Selected fundamental parameters that define the heavier pnictogen elements are summarized in Table 1.1 [4]. While arsenic and bismuth are monoisotopic, antimony exists as two substantially abundant naturally occurring isotopes. All isotopes of the heavy pnictogens are NMR active nuclei, indicating that the nuclear spin will interact with an applied magnetic field. However, as the nuclear spins of these isotopes are all quadrupolar, NMR spectra generally consist of broad peaks and provide limited information. The atoms As, Sb and Bi all have the same effective nuclear charge ( $Z_{\text{eff}} = 6.30$ , Slater), which estimates the charge

**Table 1.1** Elemental parameters for arsenic, antimony and bismuth (adapted with permission from [4]). Copyright Springer Science + Business Media

Parameter	As	Sb	Bi
Atomic Number	33	51	83
Natural Isotopes (abundance)	<sup>75</sup> As (100) Stable	<sup>121</sup> Sb (57.4) Stable <sup>123</sup> Sb (42.6) Stable	<sup>209</sup> Bi (100) $\alpha$ -decay [5] $t_{1/2}: (1.9 \pm 0.2) \times 10^{19} \text{yr}$
Radioactive Stability			
Nuclear Spin, I	-3/2	+5/2 ( <sup>121</sup> Sb) +7/2 ( <sup>123</sup> Sb)	-9/2
Ionization Energies (kJ mol <sup>-1</sup> )			
M → M <sup>+</sup>	947	833.7	703.2
M <sup>+</sup> → M <sup>2+</sup>	1798	1794	1610
M <sup>2+</sup> → M <sup>3+</sup>	2735	2443	2466
M <sup>3+</sup> → M <sup>4+</sup>	4837	4260	4372
M <sup>4+</sup> → M <sup>5+</sup>	6043	5400	5400
Electron Affinity (kJ mol <sup>-1</sup> ) M(g) → M <sup>-</sup> (g)	78	101	91.3
Electronegativity, $\chi^P$ (Pauling scale)	2.18	2.05	2.02
Atomic Radius (Å)	1.25	1.82	1.55
Single-bond Covalent Radius (Å)	1.21	1.41	1.52
Van der Waals Radius (Å)	2.00	2.20	2.40
Ionic Radii (Å)			
M <sup>5+</sup>	0.46	0.62	0.74
M <sup>3+</sup>	0.58	0.76	0.96

experienced by a valence electron taking into account shielding by the other electrons. As a consequence, the ionization energies and electron affinities for As, Sb and Bi are very similar. The ionization energy is the energy required to remove a valence electron from an atom or an ion in the gas phase. The ionization energies are predictably greater for ions with higher positive charge and are typically lower for atoms or ions with higher principal quantum number (*n*). The electron affinity is the energy released when an atom gains an electron to form an anion in the gas phase. The electronegativity ( $\chi^P$ ), defining the relative ability of an atom to attract electrons to itself in a covalent bond, is sufficiently larger for arsenic than for antimony and bismuth. The atomic radii, covalent radii and ionic radii are smallest for arsenic and largest for bismuth atoms consistent with the relative atomic mass and number of electron shells.

Selected biological and toxicity data for As, Sb and Bi are summarized in Table 1.2. While some arsenic compounds are essential to certain animal species [4], most arsenic compounds display toxic biological effects even when present in only small amounts. Some compounds, such as Salvarsan 606 [6], are therapeutic, although there are reported side effects, including death in high dosages. Neither antimony nor bismuth has any known natural biological function. While antimony has toxicity comparable with that of arsenic, bismuth can be tolerated in large quantities. Bismuth compounds have been used for more than two centuries to treat many medical disorders and are now commonly available in the preparations known commercially as Peptobismol and DeNol [3].

**Table 1.2** Biological and toxicity data for arsenic, antimony and bismuth

	As	Sb	Bi
Biological Role [4]	Essential to some species including humans; toxic; stimulatory; carcinogenic	Not essential; toxic; stimulatory	Not essential; nontoxic
Amount in Average (70 kg) Human Body (dry mass, mg) [7]	0.5–15 depending on diet	2	<0.5
Daily Dietary Intake (mg)	0.04–1.4 [4]	0.002–1.3 [4, 8]	0.005–0.02 [1]
Lethal Intake (mg/kg body weight)	1–3 inorganic [1]  500 dimethylarsinic acid [9]	0.75 mg/kg antimony potassium tartrate [1]	5–20 g/day for years [2]

## 1.2 Allotropes

Elemental antimony and bismuth are most stable in the  $\alpha$  form, which is rhombohedral and typically grey in appearance, while the most common form of arsenic is  $\beta$ -arsenic (grey arsenic). The  $\alpha$ -allotropic forms are analogous to black phosphorus, composed of layers of hexagonally connected sheets, as shown in Figure 1.1. The interatomic distances ( $r_1$ ,  $r_2$ ) are predictably larger for the heavier elements due to their larger atomic radii. The difference in the interlayer distance ( $r_2$ ) between each adjacent pnictogen atom decreases from P to As to Sb to Bi (Table 1.3).

Arsenic is observed to exist in two (yellow and black) [10, 11] additional allotropic forms, while antimony adopts five allotropes [11, 12] and bismuth adopts at least three allotropes [11]. Most of these alternate allotropes are only nominally stable or require high temperature or pressure conditions [11, 13].

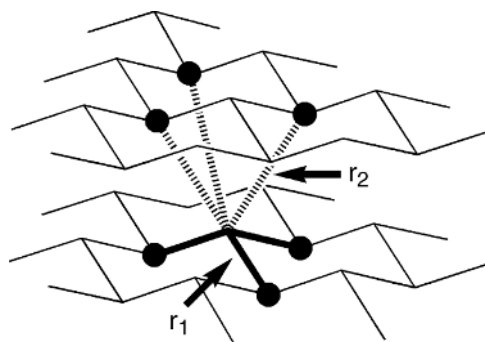


**Figure 1.1** Schematic drawing of the  $\alpha$ -rhombohedral form of elemental As, Sb or Bi,  $r_1$  is the interatomic distance within a sheet and  $r_2$  is the interlayer distance (Table 1.3)

**Table 1.3** Comparative structural parameters for  $\alpha$ -rhombohedral arsenic, antimony and bismuth at 298 K

	$r_1$ (Å)	$r_2$ (Å)	$r_2/r_1$	Angle M–M–M	References
$\alpha$ -As	2.517	3.120	1.240	$96^\circ 73'$	[14, 15]
$\alpha$ -Sb	2.908	3.355	1.153	$95^\circ 60'$	[15, 16]
$\alpha$ -Bi	3.072	3.529	1.149	$95^\circ 45'$	[15, 17]

### 1.3 Bond Energies

Arsenic, antimony and bismuth form stable covalent bonds with most elements. For direct comparison, Table 1.4 lists experimentally determined bond energies for the dissociation of selected pnictogen-element diatomic species in the gas phase. While these energies are not representative of pnictogen element bonds in larger molecules, the same relative trends are exhibited. Bond energies are dependent on the molecular environment in the specific compound studied. For a particular element, Pn-element bond energies generally decrease from As to Sb to Bi. For example, the Pn–H bonds in AsH<sub>3</sub> and SbH<sub>3</sub> are 319.2 kJ mol<sup>−1</sup> and 288.3 kJ mol<sup>−1</sup>, respectively [18]. Moreover, bonds involving lighter elements are generally stronger. For example, the Bi–X bonds in BiF<sub>3</sub> and BiBr<sub>3</sub> are 435 kJ mol<sup>−1</sup> and 297.1 kJ mol<sup>−1</sup>, respectively [18]. Similarly, in OAsPh<sub>3</sub> and SAsPh<sub>3</sub>, the As=Ch bond is 429 kJ mol<sup>−1</sup> and 293 kJ mol<sup>−1</sup>, for Ch=O and Ch=S respectively [18].

### 1.4 Oxidation States

The pnictogen elements access oxidation states ranging from −3 to +5, as summarized in Figure 1.2, which presents the relative energy of each oxidation state in volts (J C<sup>−1</sup>) and in Gibbs energy. In contrast to nitrogen and phosphorus, arsenic, antimony and bismuth thermodynamically favour the elemental form. While positive oxidation states for

**Table 1.4** Experimentally determined pnictogen-element bond energies of selected diatomic molecules in the gas phase, kJ mol<sup>−1</sup> (from reference [19])

[kJ mol <sup>−1</sup> ]	As	Sb	Bi
H	274.0 ± 2.9	239.7 ± 4.2	≤283.3
D	270.3	—	283.7
N	489 ± 2.1	460 ± 84	—
O	484 ± 8	434 ± 42	337.2 ± 12.6
F	410	439 ± 96	366.5 ± 12.5
P	433.5 ± 12.6	356.9 ± 4.2	281.7 ± 13
S	379.5 ± 6.3	378.7	315.5 ± 4.6
Cl	448	360 ± 50	300.4 ± 4.2
As	385.8 ± 10.5	330.5 ± 5.4	—
Se	96	—	280.3 ± 5.9
Br	—	314 ± 59	240.2
Sb	330.5 ± 5.4	301.7 ± 6.3	252.7 ± 3.9
I	296.6 ± 24	—	186.1 ± 5.8
Bi	—	252.7 ± 3.9	204.4

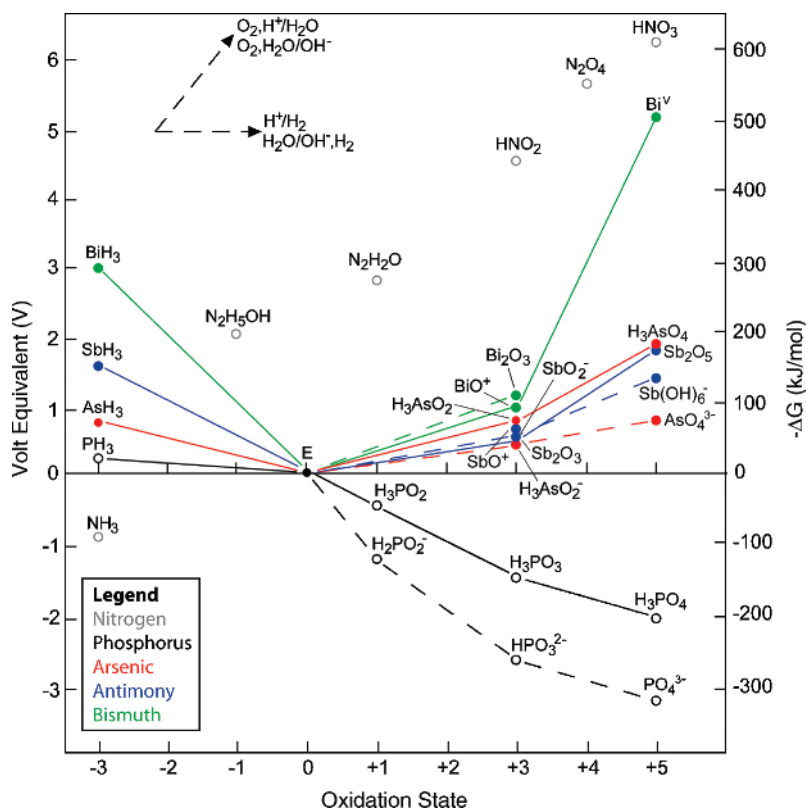


**Figure 1.2** Oxidation state diagram for the pnictogen elements. Dashed lines represent basic conditions. Solid lines represent acidic conditions. Adapted with permission from [11]. Copyright Elsevier (1997)

phosphorus are stable, compounds containing arsenic, antimony or bismuth in positive oxidation states are unstable with respect to elemental forms. This phenomenon is most dramatic when comparing the relative energy differences for compounds containing pnictogens in +5 oxidation state.

## 1.5 Relativistic Effects and Orbital Contraction

The property trends observed for the pnictogens can be rationalized by consideration of orbital contraction (for arsenic) and relativistic effects (for bismuth). The elements at the end of the third period exhibit a contraction and a more tightly bound  $ns^2$  ( $n > 3$ ) electron pair, due to a relatively high effective nuclear charge ( $Z_{\text{eff}}$ ) [20]. The electrons in the  $d$ -orbitals provide less effective screening of the nuclear charge than those in  $s$ - and  $p$ -orbitals due to the directionality and diffuse nature of the  $d$ -orbitals. This effect is most dramatic for arsenic, and rationalizes the relatively high fourth and fifth ionization energies of arsenic and antimony, since the  $ns^2$  electron pair is accordingly anomalously stabilized. Consequently, the electronegativity for arsenic is comparable to that of

phosphorus ( $\chi^{\text{P}}$ : As 2.18, P 2.19 [21];  $\chi^{\text{AR}}$ : As 2.20, P 2.06) [22] and is significantly greater than those of the heavier pnictogens. Bismuth is further affected by the contraction corresponding to the less effective screening provided by occupied *f*-orbitals.

When the velocity of an electron (*v*) (Equation 1.1) in an atom is a fraction of the speed of light (*c*), relativistic effects occur [20, 23–25]. As this velocity is directly proportional to atomic number (*Z*), these effects can generally be neglected for the lighter elements (*Z* < 79) but they dominate the chemical behaviour of the heavier elements.

$$v = [(2\pi e^2)/(nh)]Z \quad (1.1)$$

$$m = m_o[1-(v/c)^2]^{-1/2} \quad (1.2)$$

The strongest relativistic effects occur in the orbital that is closest to the highly positive nucleus, the 1*s* orbital. This results in an increase of mass (according to the special theory of relativity [26, 27] [Equation 1.2]) and corresponding reduction of the Bohr radius of the atom. In bismuth, the velocity of a 1*s* electron is 60% of the speed of light, leading to a mass of 1.26 times the rest mass (*m*<sub>o</sub>) and a 26% reduction in the radius of the 1*s* orbital. In contrast, the 1*s* radial contraction of arsenic and antimony are only 3 or 8%, respectively [28]. Accordingly, the energies of all of the *ns* orbitals in bismuth are substantially lower than those of arsenic and antimony. The *p*-orbital energies are also lower but the difference is smaller than that of the *s*-orbitals [29]. The lower energy of the valence 6*s* orbital implies that the 6*s*<sup>2</sup> lone pair of electrons is less readily available for bonding, making bismuth(III) a significantly weaker Lewis base than the lighter pnictogens and disfavours the +5 oxidation state for bismuth. In addition, the *s*-orbital is less readily available [30], so that compounds of As, Sb and Bi adopt bond angles close to 90° implicating the use of pure *p*-orbitals [31] in bonding (see also Section 1.8 – *Hybridization and Inversion*).

## 1.6 Structure and Bonding

The chemistry of a molecule is defined by the structure of the molecule and the bonding therein. Furthermore, the local structure and bonding of the feature element(s) within a molecule are particularly influential in governing reactivity. The heavy pnictogen elements are observed to adopt a wide variety of coordination numbers and geometries depending on the substituents involved. Representations of possible bonding environments for the pnictogen centre, up to a coordination number of six, are illustrated in Figure 1.3.

The low coordination numbers in bonding arrangements A and B require that the pnictogen centre engage in  $\pi$ -bonding with neighbouring atom of the substituent(s). As  $\pi$ -bonding involving elements beyond the second period of the Periodic Table is thermodynamically disfavoured with respect to  $\sigma$ -bonding [30] the presence of sterically bulky substituents is required to enable the isolation of compounds containing such bonding arrangements, as in the case of AsCMes\* (Mes\* = 2,4,6-tri-*t*-butylphenyl) [32]. Structure C represents the  $\sigma$ -bonded framework of a pnictide anion. Structure D is perhaps the most common geometry known for these elements, possessing three covalent bonds and one lone pair of electrons. Reluctance for the heavy elements to engage in hybridization (*sp* mixing)

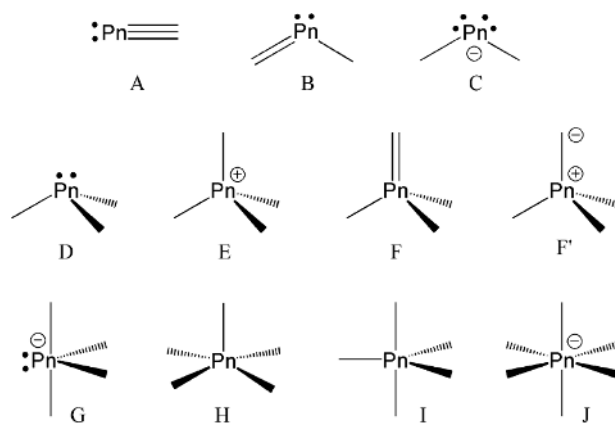


**Figure 1.3** Bonding models for possible geometries (arrangements of substituents) at the pnictogen centre for coordination numbers from 1–6

results in typical bond angles in such species approximating  $90^\circ$  (see also Section 1.8 *Hybridization and Inversion*). Nevertheless, substituent steric interactions or chelated structures can enforce other geometries. The tetracoordinate tetrahedral geometry E is common for arsenic but less evident for antimony and rare for bismuth.

Computational studies of potential bonding arrangement F suggest that d-orbital participation is minimal for the heavy elements (As, Sb, Bi), therefore, this traditional double bond arrangement is better described as a singly bonded zwitterion F' (analogous to environment E with localized negative charge at one substituent) [33]. Moreover, many derivatives adopt bridged or extended structures (see also Section 1.7 *Clusters and Extended Structures*) [34].

Structures G, H, I and J are typically associated with the +5 oxidation state. Geometries that can be described as distorted versions of H (square based pyramid) or I (trigonal bipyramid) are common due to Berry pseudo rotation between these two extremes. In geometry I and other pseudo trigonal bipyramidal arrangements, the more electronegative atoms are typically located in axial positions, barring steric constraints. In addition to the indicated geometries, bismuth can readily adopt geometries with coordination numbers even greater than six, usually with interactions to more distant ligands that are within the sum of the van der Waals radii [35, 36]. For example, nonahydratobismuth(III) triflate contains nine relatively short Bi–O bond distances at 2.45 Å (equatorial) or 2.58 Å (trigonal prism), Figure 1.4.

Common geometries for arsenic, antimony and bismuth are summarized in blue in Table 1.5, with examples of known geometries for comparison.

Pnictogen-oxygen compounds are of particular interest in a biological context and their potential structural diversity is depicted in Figure 1.5. Derivatives containing a pnictogen centre that bears a lone pair and therefore representing pnictines (arsines, stibines or bismuthines), are represented by **1** and show diversity by virtue of one, two or three alkoxide substituents. Pnictine oxides, **2**, show similar alkoxide substituent variability. Further diversity is possible for alkoxides of pentacoordinate pnictogen centers, shown in **3**, although few derivatives have been reported in the absence of chelating oxygen donors. For antimony and bismuth, the pnictine oxides and pentacoordinate alkoxides form associated arrangements

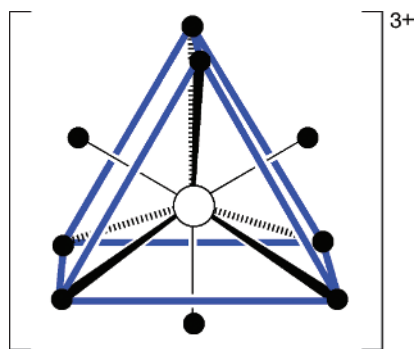


**Figure 1.4** Cation of the nonahydratobismuth(III) triflate salt, with bismuth depicted as a white circle, water molecules as black circles and the trigonal prism geometry in blue

**Table 1.5** Coordination numbers and approximate geometries for the pnictogen (Pn) centre in representative compounds

Coordination No.	Approximate geometry	Formula of representative compound	Refs
1	A	AsCMes*	[32]
2	B	[As(NMe) <sub>2</sub> C <sub>3</sub> H <sub>6</sub> ] <sup>+</sup>	[37]
	C	[SbPh <sub>2</sub> ] <sup>−</sup>	[38]
	C	[As(PR <sub>3</sub> ) <sub>2</sub> ][BPh <sub>4</sub> ]	[39]
	C	Li[AsPh <sub>2</sub> ]	[41]
3	D	AsPh <sub>3</sub>	[40]
	<b>D</b>	<b>SbR<sub>3</sub>, R=organic substituent</b>	[41]
	<b>D</b>	<b>BiMe<sub>3</sub></b>	[35]
		Bi(L-cysteine) <sub>3</sub> ·H <sub>2</sub> O	[42]
	Trigonal planar	PhSb[Mn(CO) <sub>2</sub> C <sub>p</sub> ] <sub>2</sub>	[43]
4	<b>E</b>	<b>[AsO<sub>4</sub>]<sup>3−</sup></b>	[44]
	E	[Me <sub>6</sub> As <sub>2</sub> ][OTf] <sub>2</sub>	[45]
	T-shaped	[(BIAN)As][SnCl <sub>5</sub> (THF)]	[46]
	G	PhSb[(SCH <sub>2</sub> CH <sub>2</sub> ) <sub>2</sub> O]	[41]
	G	[Ph <sub>2</sub> SbCl <sub>2</sub> ] <sup>−</sup>	[41]
	<b>G</b>	<b>[Ph<sub>2</sub>Bi(OCOFCF<sub>3</sub>)<sub>2</sub>]<sup>−</sup></b>	[35]
5	<b>I</b>	<b>(Me<sub>2</sub>C(O)CO<sub>2</sub>)<sub>2</sub>AsPh</b>	[47]
	H	Ph <sub>5</sub> Sb	[41]
	H	Ph <sub>5</sub> Bi	[35]
	I	Bi(C <sub>6</sub> H <sub>4</sub> CH <sub>3</sub> -4) <sub>3</sub> (C <sub>6</sub> H <sub>4</sub> F-2) <sub>2</sub>	[35]
	H	Bi(C <sub>6</sub> H <sub>4</sub> F-4) <sub>3</sub> (C <sub>6</sub> F <sub>5</sub> ) <sub>2</sub>	[35]
6	<b>J</b>	<b>[AsF<sub>6</sub>]<sup>−</sup></b>	[35]
	J	[Bi(Me) <sub>6</sub> ] <sup>−</sup>	[35]
7	Distorted pentagonal bipyramid	(κ <sup>2</sup> -O <sub>2</sub> CCF <sub>3</sub> ) <sub>2</sub> Ph <sub>3</sub> Bi	[35]
9	Tricapped trigonal prism	[Bi(OH <sub>2</sub> ) <sub>9</sub> ] <sup>3+</sup>	[35]
12	Icosahedral	SbRh <sub>12</sub> (CO) <sub>27</sub> <sup>3−</sup>	[48]

Approximate geometries refer to the legend in Figure 1.3 where possible and the most common coordination geometries (and associated representative compounds) for each element are highlighted in blue.  
aryl-BIAN = 1,2-bis(arylimino)acenaphthene.



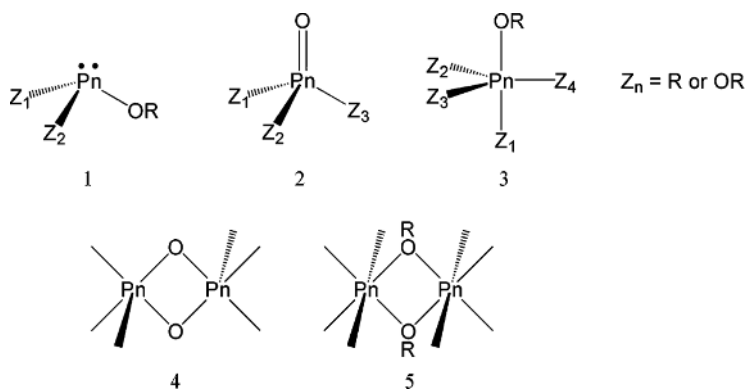


**Figure 1.5** Molecular structures for oxygen-pnictogen compounds

such as those shown in **4** and **5**, respectively. Analogous structures are extremely rare for arsenic, with only few characterized examples [49]. Occurrences of single bridging oxides between antimony and bismuth centres are also known, forming oligomers or polymers. Bismuth oxyhalides of the general formula  $\text{BiOX}$  are well known and typically adopt ionic structures containing  $[\text{Bi}=\text{O}]^+$  [50, 51]. Other chalcogen-containing species (sulfides, selenides) show similar structural features. For example,  $\text{Bi}(\text{L-cysteine})_3 \cdot \text{H}_2\text{O}$  has a trigonal pyramidal structure and contains only Bi–S metal-ligand interactions [42].

## 1.7 Clusters and Extended Structures

Pnictogen mineral oxides contain anions of the type  $\text{PnO}_4^{3-}$  (e.g., arsenate) and  $\text{PnO}_3^{3-}$  (e.g., arsenite) and adopt extended structures similar to phosphate ( $\text{PO}_4^{3-}$ ) and phosphite ( $\text{PO}_3^{3-}$ ). The common oxide of bismuth ( $\text{Bi}_2\text{O}_3$ , bismite) does not contain a molecular unit but some of the common mineral forms of arsenic (realgar and orpiment) display molecular cage structures [11], shown in Figure 1.6. Cage structures such as these recur regularly in pnictogen cluster chemistry and are analogous to the elemental cluster anions, for example  $\text{Pn}_7^{3-}$ . Bismuth is observed to form a variety of cationic element clusters of the type  $\text{Bi}_m^{n+}$ , examples of which are illustrated in Figure 1.7 [52].

The Lewis acceptor properties of antimony and bismuth are responsible for extended structures involving halogen centers in bridging positions that are analogous to the

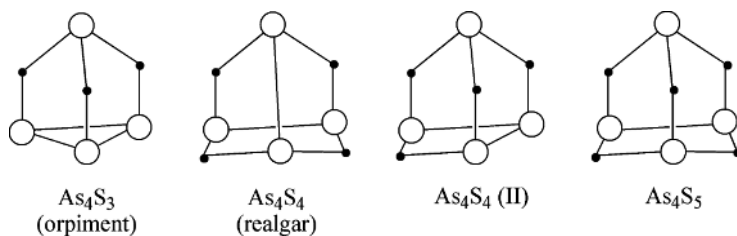


**Figure 1.6** Selected structures of  $\text{As}_m\text{S}_n$  clusters (As = white circles; S = black dots)

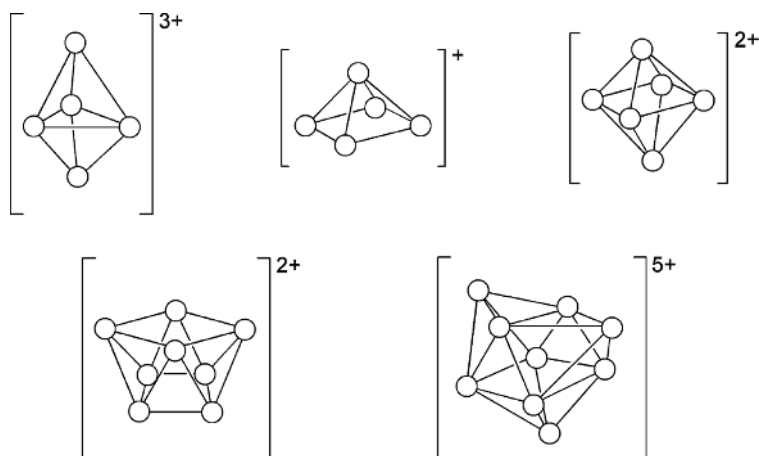


**Figure 1.7** Examples of bismuth (white circles) cluster cations, including trigonal bipyramid, square based pyramid, distorted octahedron, square antiprism, and tricapped trigonal prism

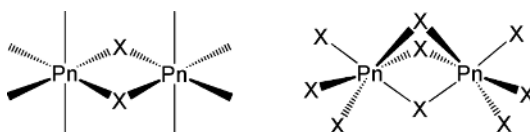


**Figure 1.8** Edge sharing and confacial bi-octahedral structures observed for antimony and bismuth (Pn) halides (X)

associated structures described above for oxides and alkoxides [12]. The two bi-octahedral frameworks (edge sharing and confacial) are shown in Figure 1.8.

Larger cage structures with multiple bridging ligands are commonly observed for bismuth [11, 41]. For example, solid state structures of medically relevant bismuth compounds with chelating ligands (citrate, subsalicylate) have recently been reported [53]. The structures of many bismuth-oxygen compounds derive from the  $[\text{Bi}_6(\text{OH})_{12}]^{6+}$  unit shown in Figure 1.9, which contains one bridging hydroxide (black dots) along each of the

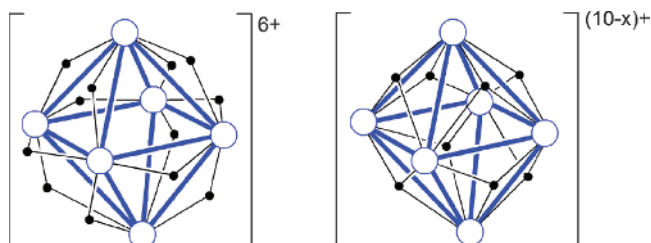


**Figure 1.9**  $[\text{Bi}_6(\text{OH})_{12}]^{6+}$  and  $[\text{Bi}_6\text{O}_x(\text{OH})_{8-x}]^{(10-x)+}$ : representative examples of bismuth (white circles) clusters, containing bridging oxygen atoms or hydroxides (black dots), with bismuth octahedra depicted in blue

12 edges of a bismuth octahedron (white circles) [11, 54]. An alternative structure [55, 56] involves bridging oxygen atoms or hydroxides on each of the eight faces of the bismuth octahedron giving formulae of the type  $[\text{Bi}_6\text{O}_x(\text{OH})_{8-x}]^{(10-x)+}$ .

The crystal structures of compounds containing a bismuth(III) atom (bearing a lone pair of 6s electrons) often reveal an empty coordination site at the bismuth centre. This structural feature has been defined as a hemidirected geometry and implicates the stereochemical activity of the lone pair at the bismuth site. This observed geometry may alternately be rationalized in terms of a *pseudotrans*-influence of ligand coordination on the bismuth centre. In the case of oxygen donors, mixing of the filled oxygen 2p and empty bismuth 6p orbitals leads to weaker ligand interactions at the coordination site opposite the oxygen atom(s); in turn, this may result in a vacant coordination site [36].

## 1.8 Hybridization and Inversion

Hybridization (or the Valence Bond Model) [30] is used extensively to rationalize the observed geometry of an atomic centre in a covalent molecule and the model is very effectively applied to most compounds containing the elements of the second period. However, the elements after neon in the Periodic Table adopt geometries that are inconsistent with the hybridization model due to the diffuse nature of *np*-orbitals relative to the *ns*-orbitals ( $n > 2$ ) and the spatial incompatibility of these orbitals relative to 2s and 2p orbitals [30]. Consequently, the heavier pnictines (Pn=P, As, Sb, and Bi) adopt bond angles close to  $90^\circ$  representing the pure *p*-orbital overlap that is responsible for the bonds to the pnictogen centre [57].

Effective hybridization by nitrogen in amines and ammonia allows vertex inversion (Figure 1.10a) to take place with a minimal energy barrier (5–6 kcal mol<sup>-1</sup>), while

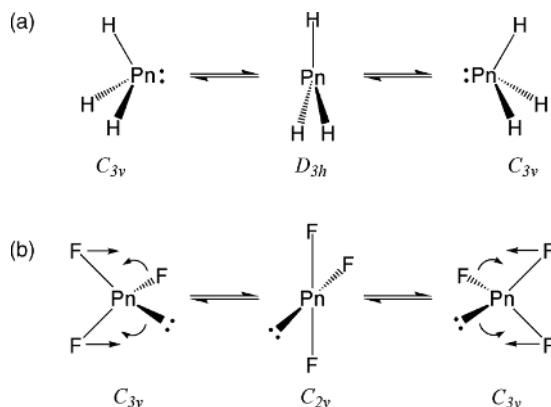


**Figure 1.10** Inversion mechanism for (a)  $\text{PnH}_3$ , vertex inversion via a trigonal planar ( $D_{3h}$ ) transition state and (b)  $\text{PnF}_3$ , edge inversion via a T-shaped ( $C_{2v}$ ) transition state. Reprinted with permission from [58]. Copyright John Wiley & Sons, Ltd

**Table 1.6** Inversion barriers for  $\text{PnH}_3$  and  $\text{PnF}_3$  ( $\text{Pn} = \text{N}, \text{P}, \text{As}, \text{Sb}, \text{Bi}$ ). Adapted with permission from [58]. Copyright John Wiley & Sons, Ltd

Inversion Barrier ( $\text{kcal mol}^{-1}$ )	Calculated	Experimental
<i>Hydrides (<math>\text{PnH}_3</math>): vertex inversion via <math>D_{3h}</math> transition state</i>		
$\text{NH}_3$	5–6	5.8
$\text{PH}_3$	35–38	31.5
$\text{AsH}_3$	39–42	—
$\text{SbH}_3$	43–48	—
$\text{BiH}_3$	61–65	—
<i>Fluorides (<math>\text{PnF}_3</math>): edge inversion via <math>C_{2v}</math> transition state</i>		
$\text{PF}_3$	53–68	
$\text{AsF}_3$	46–58	
$\text{SbF}_3$	38–47	
$\text{BiF}_3$	34–39	

phosphines, arsines, stibines and bismuthines have a substantial barrier to vertex inversion (Table 1.6). The  $D_{3h}$  transition state for inversion of a pnictine requires ammonia to adopt trigonal planar  $sp^2$  hybridization and promotion of the non-bonding (lone pair) electrons in the  $sp^3$  orbital to a  $p\pi$  orbital [58]. The energy associated with this bonding adjustment is small for nitrogen, while for the heavier pnictines the  $s$  to  $p$  promotional energy for nonhybridized orbitals is substantial. In contrast, the halopnictines undergo edge-inversion via a  $C_{2v}$  transition state as illustrated in Figure 1.10b, which exhibits an opposite trend in terms of the inversion energy barrier (Table 1.6).

## 1.9 Coordination Chemistry

The lone pair of electrons at the pnictogen centre in derivatives of  $\text{PnR}_3$  is available for bonding with a Lewis acid. The electron donating ability decreases according to  $\text{PR}_3 > \text{AsR}_3 > \text{SbR}_3 \gg \text{BiR}_3$  [28, 59]. The presence of electron donating substituents increases the basicity of the pnictogen centre and bulky substituents impose a steric shield resulting in a kinetic barrier to bond formation and a decreased basicity relative to pnictines bearing less bulky substituents. Nevertheless, heavy pnictines adopt smaller cone angles than amines, which affects their relative steric restrictions [60, 61]. According to Pearson's hard-soft acid-base theory [62], relatively soft donors favour interactions with relatively soft acceptors. For instance, coordination of an arsine to a soft metal centre is favoured over the coordination of a phosphine despite the weaker donor ability of the arsine [28].

Lewis acid behaviour is most common for compounds involving higher oxidation states and higher coordination numbers. For example, the fluoride anion forms a strong complex with  $\text{PF}_5$  and  $\text{SbF}_5$  to give  $\text{PF}_6^-$  and  $\text{SbF}_6^-$ , respectively. Although pnictines are more traditionally described as Lewis bases with reference to their available lone pair, complexes of pnictines as Lewis acids are known. Introduction of both a formal positive charge and an open coordination site in pnictogenium cations,  $\text{PnR}_2^+$ , results in their extensive chemistry as Lewis acids [45, 63].

**Table 1.7** Geological Data (adapted with permission from [4]. Copyright Springer Science + Business Media)

Abundance	As	Sb	Bi
Earth: Crust	1.5 ppm [7] 3.4 ppm [1]	0.2–0.5 mg/kg [1]	0.048 ppm [7]
Soil (mg/kg dry wt.)	*Average range 4.8–13.6 [9] 0.1–10 [1]	$1 \times 10^{-3}$ [1] Up to 10 nmol/g bound to humic acids stibnite [Sb <sub>2</sub> S <sub>3</sub> ] ullmanite [NiSbS]	bismite [ $\alpha$ -Bi <sub>2</sub> O <sub>3</sub> ] bismuthinite [Bi <sub>2</sub> S <sub>3</sub> ] bismutite [(BiO) <sub>2</sub> CO <sub>3</sub> ] main source is by-product from Pb and Cu smelters
Chief ores and sources	up to 90 nmol/g bound to humic acids realgar [As <sub>4</sub> S <sub>4</sub> ] orpiment [As <sub>2</sub> S <sub>3</sub> ] loellingite [FeAs <sub>2</sub> ]		
Seawater (ppm)			
Atlantic surface	$1.45 \times 10^{-3}$	c. $0.3 \times 10^{-3}$	$5.1 \times 10^{-8}$
Atlantic deep	$1.53 \times 10^{-3}$	—	n.a.
Pacific surface	$1.47 \times 10^{-3}$	—	$4 \times 10^{-8}$
Pacific deep	$1.75 \times 10^{-3}$	—	$0.4 \times 10^{-8}$
Residence time in ocean (years) (oxidation state in parentheses)	90 000 (V)	c. $3.5 \times 10^5$ (III)	n.a. (III)
*Freshwater [8, 9]			
Surface water	Average 1.6 µg/l; ranges from 0.1–25.0 µg/l	<10 µg/l; ranges from 0.001–9.1 mg/l	—
Ground water and deep lake sediments	Average 1.5 µg/l; ranges from 0.1–60 µg/l	<5 µg/l	—
*Air (ng/m <sup>3</sup> )	Average 1; ranges from 0.5–17 (urban) [9]	0.11–0.23 (urban) [1]	1–66 (urban) [1]
			0.1–0.6 (rural) [1]

Values marked with \* indicate geological data from Canada, while remaining values are nonspecific global data.

## 1.10 Geological Occurrence

The natural abundance in land and water sources of arsenic is significantly greater than that of antimony or bismuth (where bismuth has the lowest natural abundance). The most common ores of arsenic are realgar ( $\text{As}_4\text{S}_4$ ), orpiment ( $\text{As}_2\text{S}_3$ ), arsenolite ( $\text{As}_2\text{O}_3$ ), arsenopyrite ( $\text{FeAsS}$ ) and enargite ( $\text{Cu}_3\text{AsS}_4$ ) [4, 64]. Arsenic is typically introduced into the biosphere in bioavailable non-mineral forms through the industrial processing of ores, improper handling of wastes, as well as use in herbicides and pesticides that are now banned in North America [9].

The common ores of antimony are stibnite ( $\text{Sb}_2\text{S}_3$ ), ulmanite ( $\text{NiSbS}$ ), livingstonite ( $\text{HgSb}_4\text{S}_8$ ), tetrahedrite ( $\text{Cu}_3\text{SbS}_3$ ) and jamesonite ( $\text{FePb}_4\text{Sb}_6\text{S}_{14}$ ) [64]. Antimony is most commonly introduced to the biosphere via natural biological and geochemical cycling processes [65]. The low aqueous solubility of antimony relative to arsenic [1] hinders its transport and bioaccumulation does not occur [8]. Only tartar emetic (antimony potassium tartrate,  $\text{C}_8\text{H}_4\text{K}_2\text{O}_{12}\text{Sb}_2 \cdot 3\text{H}_2\text{O}$ ) has high water solubility (83 g/l) [1]. Dissolved antimony discharged into the natural aquifer typically precipitates as  $\text{Sb}_2\text{O}_3$  or  $\text{Sb}_2\text{O}_5$  [8].

Bismuth occurs in the ore bismite ( $\alpha\text{-Bi}_2\text{O}_3$ ), bismuthinite ( $\text{Bi}_2\text{S}_3$ ) and bismuthite ( $\text{BiO})_2\text{CO}_3$  [64]. Most bioavailable bismuth has been introduced via human activity; however, small amounts may be released due to volcanic activity or aqueous action [64]. Table 1.7 provides geological and environmental abundance data for these heavier pnictogens.

## 1.11 Aqueous Chemistry and Speciation

The dominant forms of arsenic in dilute aqueous solutions are  $\text{As}(\text{OH})_3$ ,  $[\text{As}(\text{OH})_4]^-$ ,  $[\text{AsO}_2(\text{OH})]^{2-}$  and  $[\text{AsO}_3]^{3-}$ , where  $\text{As}(\text{OH})_3$  behaves as a Lewis acid and can form adducts in aqueous media. Oxygen exchange between water molecules and arsenite anions is catalysed by trace amounts of  $[\text{H}_2\text{AsO}_3]^-$  [65]. In both acidic and basic environments, arsenic is commonly methylated [64] as  $[\text{MeAsO}_4]^{2-}$ ,  $[\text{Me}_2\text{AsO}_2]^-$  and  $\text{Me}_3\text{AsO}$  [9]. Arsenobetaine and arsenocholine (Figure 1.11) are the common forms of arsenic in marine organisms and are found to be nontoxic in mice and hamsters [66]. In general, inorganic forms of arsenic have higher toxicity in humans than organoarsines [64], which are readily excreted [1, 9].

Antimony occurs most commonly as  $[\text{Sb}(\text{OH})_6]^-$ , although it has also been postulated as  $\text{Sb}(\text{OH})_5 \cdot \text{H}_2\text{O}$  in aqueous environments at  $\text{pH} > 4$  [65]. Under acidic conditions ( $\text{pH} 2$ ),  $[\text{SbO}]^+$  or  $[\text{Sb}(\text{OH})_2]^+$  are found [12, 65], while at  $\text{pH} > 11$ ,  $[\text{Sb}(\text{OH})_4]^-$  is the dominant form [65]. Bismuth has a diverse aqueous chemistry analogous to arsenic. The dominant species observed in natural waters is  $\text{Bi}(\text{OH})_3$  [67].

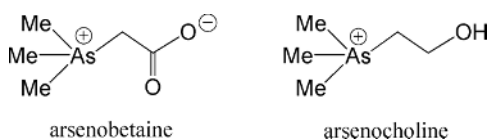


**Figure 1.11** Molecular structures of the nontoxic forms of arsenic in marine organisms

## 1.12 Analytical Methods and Characterization

Due to the quadrupolar nuclear spins (Table 1.1) of the heavy pnictogen elements, they are not readily analysed by NMR spectroscopy, one of the most versatile methods of characterization. X-ray diffraction can provide the most definitive characterization data for compounds of these elements, if crystalline samples [68] are available, although powder diffraction data [69] also yields useful information. Infrared [70] and Raman [71] vibrational spectroscopy of solids and solutions, as well as UV-visible absorbance [72] spectroscopy of solutions, have been employed to elucidate structural information. Mass spectrometry [73] has also been employed to determine the formula of ions in the gas phase. Antimony-121 ( $^{121}\text{Sb}$ ) can be analysed by Mössbauer spectroscopy [74, 75] giving both structural (e.g., molecular symmetry and lone pair orientation) and electronic information (e.g., oxidation state, electronic configuration, bond ionicity and orbital population analysis with respect to calculated orbitals).

## 1.13 Conclusions

Arsenic, antimony and bismuth display a diverse chemistry that is distinct from that of their lighter congeners in Group 15. Furthermore, the relative instability of the +5 oxidation state for arsenic and bismuth and the tendency of antimony and bismuth to form extended molecular structures distinguish these elements from one another. The resulting coordination environments preferred by these elements leads to structural features that may prove significant in biological and medicinal contexts.

## References

1. Nordberg, G.F., Fowler, B.A., Nordberg, M. and Friberg, L. (eds) (2007) *Handbook on the Toxicology of Metals*, Elsevier, Burlington.
2. Seiler, H.G., Sigel, A. and Sigel, H. (eds) (1994) *Handbook on Metals in Clinical and Analytical Chemistry*, Marcel Dekker, New York.
3. Briand, G.G. and Burford, N. (1999) *Chemical Reviews*, **99**, 2601–2657.
4. Norman, N.C. (ed.) (1998) *Chemistry of Arsenic, Antimony and Bismuth*, Blackie Academic and Professional, London.
5. de Marcillac, P., Coron, N., Dambier, G. *et al.* (2003) *Nature*, **422**, 876–878.
6. Lloyd, N.C., Morgan, H.W., Nicholson, B.K. and Ronimus, R.S. (2005) *Angewandte Chemie-International Edition*, **44**, 941–944.
7. Emsley, J. (1998) *The Elements*, Oxford University Press, Inc., New York.
8. Health Canada (1999) *Guidelines for Canadian Drinking Water Quality - Supporting Documentation - Antimony*, Water Quality and Health Bureau, Healthy Environments, and Consumer Safety Branch, Health Canada, Ottawa.
9. Health Canada (2006) *Guidelines for Canadian Drinking Water Quality: Technical Document - Arsenic*, Water Quality and Health Bureau, Healthy Environments, and Consumer Safety Branch, Health Canada, Ottawa.
10. Smith, P.M., Leadbetter, A.J. and Apling, A.J. (1975) *Philosophical Magazine*, **31**, 57–64.
11. Greenwood, N.N. and Earnshaw, A. (1997) *Chemistry of the Elements*, Butterworth-Heinemann, Oxford.

12. King, R.B. (1994) in: *The Encyclopedia of Inorganic Chemistry* (ed. R.B. King), John Wiley & Sons, Canada Ltd Toronto, pp. 170–176.
13. Sisler, H.H. (1988) in: *Inorganic Reactions & Methods* (eds J.J. Zuckermann and A.P. Hagen), Wiley-VCH Verlag GmbH Weinheim, pp. 30–31.
14. Schiferl, D. and Barrett, C.S. (1969) *Journal of Applied Crystallography*, **2**, 30–36.
15. Group V. (1982) in: *The Structure of the Elements* (ed. J. Donohue), John Wiley & Sons, Inc., New York, pp. 280–316.
16. Barrett, C.S., Cucka, P. and Haefner, K. (1963) *Acta Crystallographica*, **16**, 451–453.
17. Cucka, P. and Barrett, C.S. (1962) *Acta Crystallographica*, **15**, 865–872.
18. Luo, Y.-R. (2007) *Comprehensive Handbook of Chemical Bond Energies*, CRC Press, Boca Raton.
19. Lide, D.R. (ed.) (2008) *CRC Handbook of Chemistry and Physics*, CRC Press, Boca Raton.
20. Baerends, E.J., Schwarz, W.H.E., Schwerdtfeger, P. and Snijders, J.G. (1990) *Journal of Physics B-Atomic Molecular and Optical Physics*, **23**, 3225–3240.
21. Pauling, L. (1932) *Journal of the American Chemical Society*, **54**, 3570–3582.
22. Allred, A.L. and Rochow, E.G. (1958) *Journal of Inorganic & Nuclear Chemistry*, **5**, 264–268.
23. Schwarz, W.H.E., Chu, S.Y. and Mark, F. (1983) *Molecular Physics*, **50**, 603–623.
24. Christiansen, P.A. and Ermler, W.C. (1985) *Molecular Physics*, **55**, 1109–1110.
25. Najafpour, M.M. (2007) *Chemical Education*, **12**, 142–149.
26. Einstein, A. (1918) *Annals of Physics*, **55**, 241–244.
27. Wereide, T. (1923) *Physical Review*, **21**, 391–396.
28. Lange, K.C.H. and Klapötke, T. (1994) in: *The Chemistry of Organic Arsenic, Antimony and Bismuth* (ed. S. Patai), John Wiley & Sons, Ltd, Chichester, pp. 315–366.
29. Thayer, J.S. (2005) *Journal of Chemical Education*, **82**, 1721–1727.
30. Kutzelnigg, W. (1984) *Angewandte Chemie-International Edition*, **23**, 272–295.
31. Pytko, P. (1988) *Chemical Reviews*, **88**, 563–594.
32. Märkl, G. and Sejpka, H. (1986) *Angewandte Chemie-International Edition*, **25**, 264–265.
33. Ferguson, G., Glidewell, C., Kaitner, B. *et al.* (1987) *Acta Crystallographica*, **C43**, 824–826.
34. Pebler, J., Weller, F. and Dehnicke, K. (1982) *Zeitschrift für Anorganische und Allgemeine Chemie*, **492**, 139–147.
35. Suzuki, H. and Matano, Y. (2001) *Organobismuth Chemistry*, Elsevier, Netherlands.
36. Payne, D.J., Egde, R.G., Walsh, A. *et al.* (2006) *Physical Review Letters*, **96**, 157403(–1)–157403(–4).
37. Burford, N., Macdonald, C.L.B., Parks, T.M. *et al.* (1996) *Canadian Journal of Chemistry*, **74**, 2209–2216.
38. Bartlett, R.A., Dias, H.V.R., Hope, H. *et al.* (1986) *Journal of the American Chemical Society*, **108**, 6921–6926.
39. Barnham, R.J., Deng, R.M.K., Dillon, K.B. *et al.* (2001) *Heteroatom Chemistry*, **12**, 501.
40. Mazhar-Ul-Haque, Tayim, H.A. and Horne, W. (1985) *Journal of Crystallographic and Spectroscopy: Resolution*, **15**, 561–571.
41. Sowerby, D.B. (1994) in: *The Chemistry of Organic Arsenic, Antimony and Bismuth* (ed. S. Patai), John Wiley & Sons, Ltd, Chichester, pp. 25–88.
42. Wang, Y.-J. and Xu, L. (2008) *Journal of Inorganic Biochemistry*, **102**, 988–991.
43. Cotton, F.A., Wilkinson, G., Murillo, C.A. and Bochmann, M. (1999) *Advanced Inorganic Chemistry*, John Wiley & Sons, Inc., New York.
44. Sorribas, V. and Villa-Bellosta, R. (2008) *Toxicology and Applied Pharmacology*, **232**, 125–134.
45. Conrad, E.D., Burford, N., McDonald, R. and Ferguson, M.J. (2008) *Inorganic Chemistry*, **47**, 2952–2954.
46. Reeske, G., Hoberg, C.R., Hill, N.J. and Cowley, A.H. (2006) *Journal of the American Chemical Society*, **128**, 2800–2801.
47. Holmes, R.R., Day, R.O. and Sau, A.C. (1985) *Organometallics*, **4**, 714–720.
48. Vidal, J.L. and Troup, J.M. (1981) *Journal of Organometallic Chemistry*, **213**, 351–363.
49. Haase, W. (1974) *Chemische Berichte*, **107**, 1009–1018.
50. Whitmire, K.H. (1998) in: *The Encyclopedia of Inorganic Chemistry* (ed. R.B. King), John Wiley & Sons, Canada Ltd, Toronto, pp. 280–291.



51. Whitmire, K.H. (1998) in: *The Encyclopedia of Inorganic Chemistry* (ed. R.B. King), John Wiley & Sons, Canada Ltd, Toronto, pp. 292–300.
52. Ruck, M. and Hampel, S. (2002) *Polyhedron*, **21**, 651–656.
53. Ge, R. and Sun, H. (2007) *Accounts of Chemical Research*, **40**, 267–274.
54. Maroni, V.A. and Spiro, T.G. (2009) *Inorganic Chemistry*, **7**, 183–188.
55. Henry, N., Mentre, O., Abraham, F. et al. (2006) *Journal of Solid State Chemistry*, **179**, 3087–3094.
56. Sundvall, B. (1983) *Inorganic Chemistry*, **22**, 1906–1912.
57. Glaesinger, W.S., Chung, Y.S. and Balasubramanian, K.J. (1993) *Chemical Physics*, **98**, 8859–8869.
58. Nagase, S. (1994) in: *The Chemistry of Organic Arsenic, Antimony and Bismuth Compounds* (ed. S. Patai), John Wiley & Sons, Ltd, Chichester, pp. 1–24.
59. Carmalt, C.J. and Norman, N.C. (1998) in: *Chemistry of Arsenic, Antimony and Bismuth* (ed. N.C. Norman), Blackie Academic and Professional, London, pp. 1–38.
60. Imyanitov, N.S. (1985) *Koordinatsionnaya Khimiya*, **11**, 1041–1045.
61. Imyanitov, N.S. (1985) *Koordinatsionnaya Khimiya*, **11**, 1171–1178.
62. Pearson, R.G. (1968) *Journal of Chemical Education*, **45**, 581–587.
63. Ellis, B.D. and Macdonald, C.L.B. (2007) *Coordination Chemistry Reviews*, **251**, 936–973.
64. Reglinski, J. (1998) in: *Chemistry of Arsenic, Antimony and Bismuth* (ed. N.C. Norman), Blackie Academic and Professional, London, pp. 403–440.
65. Richens, D.T. (1997) *The Chemistry of Aqua Ions*, John Wiley & Sons, Ltd, Chichester.
66. Maeda, S. (1994) in: *The Chemistry of Organic Arsenic, Antimony and Bismuth Compounds* (ed. S. Patai), John Wiley & Sons, Ltd, Chichester, pp. 725–759.
67. Stumm, W. and Morgan, J.J. (1996) *Aquatic Chemistry: Chemical Equilibria and Rates in Natural Waters*, John Wiley & Sons, Inc., New York.
68. Massa, W. (2004) *Crystal Structure Determination*, Springer, New York.
69. David, W.I.F., Shankland, K., McCusker, L.B. and Baerlocher, Ch. (eds) (2002) *Structure Determination from Powder Diffraction Data*, Oxford University Press, Oxford.
70. Griffiths, P.R. and de Haseth, J.A. (2007) *Fourier Transform Infrared Spectroscopy*, John Wiley & Sons, Inc., Hoboken.
71. Smith, E. and Dent, G. (2005) *Modern Raman Spectroscopy, A Practical Approach*, John Wiley & Sons, Inc., Hoboken.
72. Perkampus, H.-H. (1992) *UV-Vis Spectroscopy and its Applications*, Springer-Verlag, Berlin.
73. Becker, J.S. (2007) *Inorganic Mass Spectrometry, Principles and Applications*, John Wiley & Sons, Inc., Hoboken.
74. Bowen, L.H. (1973) in: *Mössbauer Effect Data Index, Covering the 1972 Literature* (eds J.G. Stevens and V.E. Stevens), Plenum, New York, pp. 71–110.
75. Stevens, J.G. (1984) in: *Chemical Mössbauer Spectroscopy* (ed. R.H. Herber), Plenum, New York, pp. 319–342.

